Absence of magnetic-field-induced effects in the mid-infrared transmission of $La_{2-x}Sr_xCuO_4$ thin films

S. V. Dordevic* and L. W. Kohlman
Department of Physics, The University of Akron, Akron, Ohio 44325, USA

L. C. Tung and Y.-J. Wang
National High Magnetic Field Laboratory, Tallahassee, Florida, 32310, USA

A. Gozar, G. Logvenov, and I. Bozovic
Department of Condensed Matter Physics and Materials Science, Brookhaven National Laboratory, Upton, New York 11973, USA
(Received 4 December 2008; revised manuscript received 22 February 2009; published 2 April 2009)

We report magnetotransmission measurements on a series of $La_{2-x}Sr_xCuO_4$ thin films. The measurements were performed in magnetic fields of 18 T, on films with doping levels of $x=0$, 0.01, 0.03, 0.045, 0.06, 0.08, and 0.10. In addition, an optimally doped film ($x=0.16$) was studied in magnetic fields up to 33 T, both above and below its superconducting critical temperature $T_c=41$ K. A combination of Gaussian and wavelet filtering was employed to improve the signal-to-noise ratio of the data. However, even after this procedure, we could not detect any field-induced changes of transmission in any of the studied samples. Our results therefore rule out a direct relation between intensity changes in mid-infrared charge excitations and a bosonic mode in the far infrared. We discuss these observations in the context of existing proposals regarding the nature of medium energy range excitations in the cuprates.

DOI: 10.1103/PhysRevB.79.134503 PACS number(s): 74.25.Gz, 74.72.Dn

I. INTRODUCTION

The mechanism of superconductivity in the cuprates continues to evade resolution. In particular, the origin of possible bosonic mode(s) responsible for pairing has been at the center of condensed matter research for the past several years.[1–4] Infrared (IR) spectroscopy was the first experimental technique to suggest that, in addition to low energy excitations, medium energy range (between 0.1–0.5 eV) and high-energy excitations (between approximately 0.5–1 eV) might also play an important role in the cuprates.[4–9] These excitations show up as modes in the optical functions, such as the quasiparticle scattering rate $1/\tau(\omega)$ or the optical self-energy $\Sigma^{op}(\omega)$.[8] In the last few years advances in angle resolved photoemission spectroscopy (ARPES) have allowed reliable studies of cuprates in the medium, and even high-energy ranges.[10–13] ARPES has also revealed excitations in these parts of the spectra, which might play an important role in high-temperature superconductivity.

It is unlikely that the medium and high-energy range excitations can have lattice origin;[14] phonon modes in the cuprates are typically confined to lower energies (below about 1000 cm^{-1}), and second-order phonons are believed to be too weak to have prominent effects on electronic properties. It is therefore natural to assume that these excitations have electronic and/or spin degrees of freedom involved. Indeed, advances in sample synthesis have allowed (relatively) large samples to be grown, which on the other hand have permitted inelastic neutron-scattering (INS) experiments to be performed in the medium energy range (as high as 200 meV).[15–19] These measurements have also detected medium energy range excitations and have assigned them to spin fluctuations or spin/charge stripes. It is not clear at the moment if or how these excitations are related to charge dynamics and, ultimately, to high-temperature superconductivity.

In this study we have used both the 18 T superconducting magnet and the 33 T resistive magnet at the National High Magnetic Field Laboratory (NHMFL) in Tallahassee, Florida to systematically investigate effects of external magnetic field on the optical properties of $La_{2-x}Sr_xCuO_4$ (LSCO) family in the mid-infrared energy range. Our measurements extend previous magnetoreflection studies[20–23] to higher magnetic fields, as well as doping ranges which were previously not examined. Within the error bars of the experiments, we do not find any field-induced changes of transmission in any of the samples, irrespective of the doping level and temperature. These results preclude an interpretation in terms of the scattering-rate-induced changes in the strength of mid-IR excitations due to coupling to a bosonic mode in the far IR, which is known to be very susceptible to external magnetic field.[24,25]

The paper is organized as follows. First, in Sec. II we describe the sample growth and magnetotransmission experiments used to study LSCO samples. In Sec. III we present the results of our optics measurements. Then, in Sec. IV we outline the numerical procedure for improving the signal-to-noise ratio in the data. The procedure consists of combined Gaussian and wavelet filtering and is shown to give good results. In Sec. V we discuss our findings in the context of current understanding of high-T_c cuprates and, in particular, the mid-energy range excitations. Finally, in Sec. VI we summarize our results.

II. EXPERIMENTS

We have measured magnetotransmission properties of several LSCO films grown on $LaSrAlO_4$ (LSAO) substrate, with doping levels of $x=0$, 0.01, 0.03, 0.045, 0.06, 0.08,

TABLE I. Parameters of $La_{2-x}Sr_xCuO_4$ films used in this study: x - doping level, ML - number of monolayers (1 ML is 6.5 Å thick), d thickness, T_N-Néel temperature (Ref. 28), T_c-superconducting temperature, and H_{c2}-upper critical field (Refs. 29 and 30).

x	0.0	0.01	0.03	0.045	0.06	0.08	0.10	0.16
ML	80	120	120	80	86	83	120	120
d (Å)	520	780	780	520	559	539.5	780	780
T_N (K)	310	215						
T_c (K)					<5	~15	~20	41
H_{c2} (T)					~20	~40	~50	~60

0.10, and 0.16. All films were grown on commercially available 0.5-mm-thick LSAO substrates, using molecular-beam epitaxy.[26] The films have different thicknesses ranging from 520 to 780 Å.[27] Some physical parameters of studied films are shown in Table I. The samples were characterized using a number of techniques such as atomic force microscopy (AFM), reflection high-energy electron diffraction (RHEED), and resistivity and magnetization measurements, all of which indicate excellent film quality.[26,31–33] Figure 1(a) displays a schematic phase diagram of LSCO, as well as the points (stars and pentagons) for which the field data were taken. Note that the doping range spans all the important parts of the phase diagram up to the optimal doping, including two antiferromagnetic films (with $x=0$ and 0.01) and several superconducting films ($x=0.06$, 0.08, and 0.10).

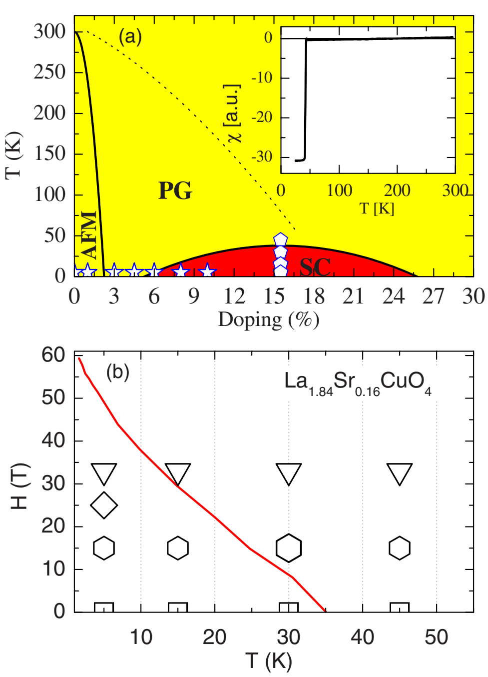

FIG. 1. (Color online) (a) Schematic phase diagram of $La_{2-x}Sr_xCuO_4$ high-temperature superconductor. The stars represent the doping levels for which magnetotransmission measurements in 18 T were performed. The pentagons represent the temperature points for which magnetotransmission measurements on an optimally doped sample were performed in 33 T. The inset shows magnetization $\chi(T)$ for this optimally doped film ($x=0.16$). A sharp transition to superconducting state occurs at $T_c=41$ K. (b) *T-H* phase diagram of optimally doped LSCO bulk sample with $T_c \simeq 38$ K, as adopted from Ref. 29. The line shown is the so-called mean-field upper critical field H_{c2}, obtained from resistivity measurements. The triangles represent *T-H* points for which magnetotransmission measurements have been performed in a 33 T field; the data are shown in Fig. 4.

The magnetotransmission measurements were performed at a temperature of 5 K in magnetic fields up to 18 T applied along the c axis (perpendicular to CuO_2 planes). In addition, an optimally doped film with $x=0.16$ and $T_c=41$ K was studied in perpendicular fields up to 33 T, both below and above T_c. The focus of the study was on the mid-IR frequency range, from approximately 1100 cm^{-1} (0.137 eV) to 3500 cm^{-1} (0.434 eV). The LSAO substrate limits the transmission at lower frequencies (because of the strong IR active phonons[34–36]), and the optical system with light pipes employed in this study renders the signal unmeasurably small at higher energies. Fortunately, the allowed frequency interval matches approximately the medium energy range, where various features have been observed in IR, ARPES, and INS.

III. RESULTS

The measurements were performed with a Fourier transform infrared spectrometer Bruker 113, coupled to a 18 T superconducting magnet. Figure 2 shows the raw transmission data for all measured samples. Transmission curves look qualitatively similar, but we note progressive suppression of transmission with strontium doping. The absolute values of transmission in the mid IR are determined primarily by the film thickness and their conductivity (i.e., doping level).[37]

Figure 3 shows the transmission ratios at 5 K for a series of LSCO films $T(\omega,18T)/T(\omega,0T)$ [along the stars in Fig. 1(a)]. Panel 3(a) displays the transmission ratio of a bare LSAO substrate. Within the error bars the ratio is unity, indicating the absence of any field-induced effects.[38] This is not unexpected and indicates that any possible field-induced changes in LSCO/LSAO samples can be ascribed to the LSCO films. Panels 3(b) and 3(c) display transmission ratios for antiferromagnetically ordered films with $x=0$ and 0.01. For these two samples, we did not detect any field-induced effects within the error bars of experiment. The next two samples (with $x=0.03$ and 0.045) are neither AFM nor superconducting and also did not show any field-induced effects [Figs. 3(d) and 3(e)]. The error bars of the measurements on the 0.045 sample were larger than for the other samples, but we emphasize that the slope of the curve shown

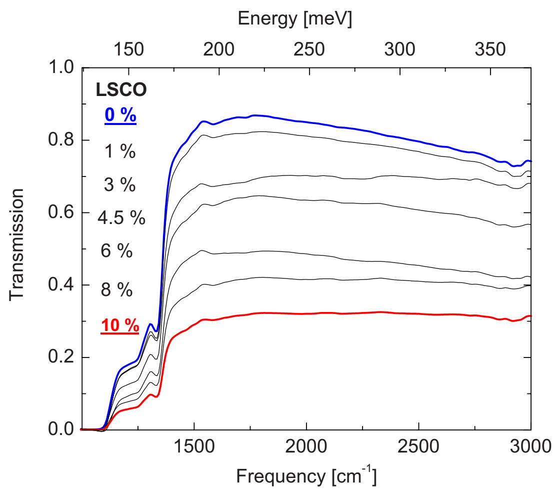

FIG. 2. (Color online) Transmission data in zero magnetic field and at $T=5$ K for LSCO films with different doping levels, from $x=0$ to $x=0.10$.

is not reproducible and, therefore, is not real. Finally, the last three measured samples ($x=0.06$, 0.08, and 0.1) are superconductors, and the measurements were performed at 5 K in the superconducting state (see Table I for their T_c's). However, in neither of the samples could we detect any field-induced effects [Figs. 3(f)–3(h)]. In particular, we did not observe any *systematic* changes as a function of doping, or development of *structures* in the mid-IR transmission within the error bars of experiment. We estimate those to be on the order of $\pm 1\%$, except for the $x=0.045$ sample.

All of the measurements in the 18 T magnet were done at 5 K. For superconducting samples this is in the superconducting state (Table I). In order to check if any field-induced effects could be detected when crossing to the normal state, we performed magnetotransmission measurements on an optimally doped film ($x=0.16$) at temperatures both below and above its critical temperature. The measurements were also

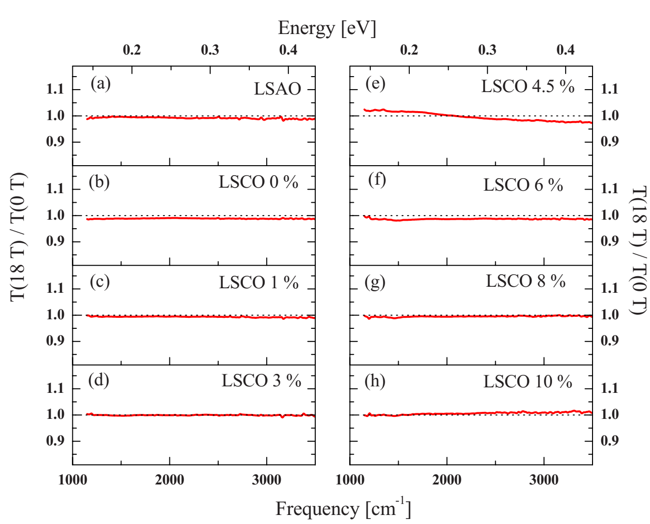

FIG. 3. (Color online) Transmission ratios $T(\omega,18)/T(\omega,0T)$ at $T=5$ K for LSCO films with different doping levels [along the stars in Fig. 1(a)]. Within the error bars of the experiment, we do not detect any field-induced changes in transmission.

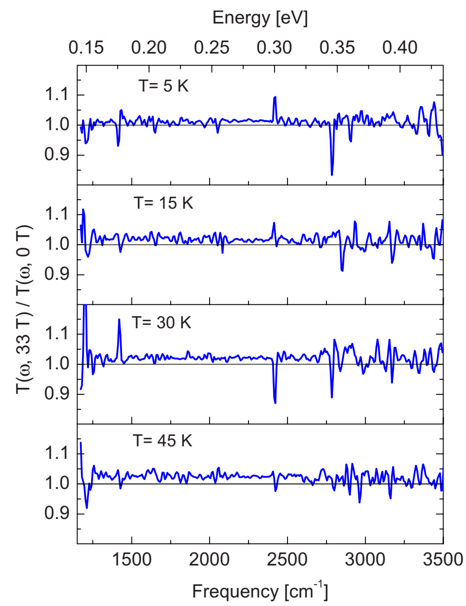

FIG. 4. (Color online) Magnetotransmission ratios $T(\omega,33T)/T(\omega,0T)$ for the optimally doped LSCO film with $T_c=41$ K at $T=5$, 15, 30, and 45 K [along the triangles in Fig. 1(b)].

performed at the NHMFL, with a Fourier transform infrared spectrometer Bruker 113, coupled to a 33 T resistive magnet. This configuration allows measurements to be performed not only at higher magnetic fields but also at elevated temperatures. Measurements at higher temperatures they are important because the upper critical field is lower, thus allowing us to probe the field-induced changes closer to the normal state. Figure 1(b) represents a *T-H* diagram of optimally doped LSCO determined from transport properties of bulk LSCO samples.[29] The symbols (squares, hexagons, diamonds, and triangles) are the *T-H* points at which transmission data were collected. In this paper we only show the results along the triangles; similar results were obtained at other data points.

Figure 4 presents the magnetotransmission ratios in 33 T $T(\omega,33T)/T(\omega,0T)$ at $T=5$, 15, 30, and 45 K [along the triangles in Fig. 1(b)]. Overall, the signal-to-noise ratios of these curves are much lower than those in Fig. 3 because of various electrical and mechanical oscillations in the system. To improve the signal-to-noise ratio, we utilized signal processing procedures.

IV. DENOISING PROCEDURE

In this section we propose a *combination* of statistical data analysis techniques, with the purpose of suppressing the noise in 33 T data. First we plot the magnetotransmission ratios on the so-called normal probability plot.[39] The normal probability plot is a graphical technique for assessing to what extent is a data set normally distributed. The data are plotted against a theoretical normal (Gaussian) distribution in such a way that the points should form an approximate straight line. Departures from this straight line indicate departures from normality.

Figure 5 displays the normal probability plot of field ratios in 33 T (from Fig. 4). As can be seen from Fig. 5 all four

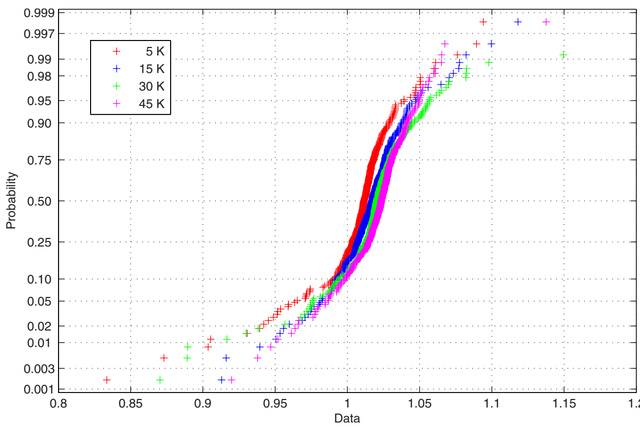

FIG. 5. (Color online) Normal probability plots for the data from Fig. 4. Note that all four curves (for all four temperatures) have the same shape. In all four cases, the data do approximately follow straight lines, which indicates that they do follow a Gaussian distribution.

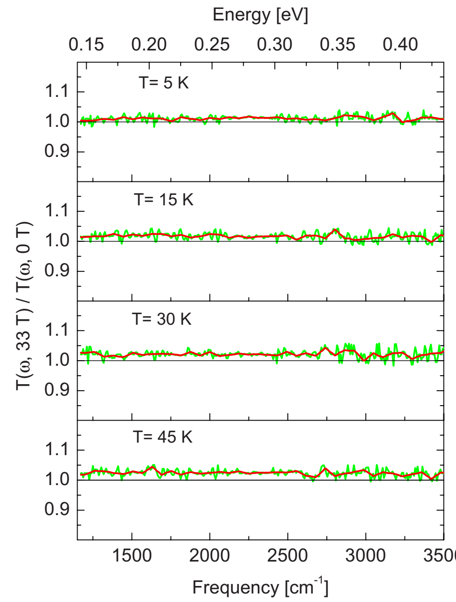

FIG. 6. (Color online) Magnetotransmission ratios $T(\omega,33T)/T(\omega,0T)$ from Fig. 4 after the removal of outliers (green lines) and after wavelet filtering (red lines).

ratios do approximately follow normal distribution (note the y axis) as most of the data points fall close to straight lines (different for different temperatures). Some points are markedly off the line, and they are called the outliers. Outliers in the data indicate the presence of factors causing nonrandom (non-Gaussian) noise in the system. In our case they come primarily from two sources: mechanical oscillations caused by flowing cooling water in the resistive magnet and by 60 Hz noise from the power lines.

The next step in the procedure is to eliminate the outliers. This was done by replacing the corresponding points in the ratios with mean values. We emphasize that the mean value for each ratio was calculated *without* the outliers: only the points inside the interval $(\mu-2\sigma,\mu+2\sigma)$ were taken into account (μ is the mean and σ is the standard deviation). This procedure preserves approximately 95% of the points, removing about 5%.[39] The results are shown with green lines in Fig. 6.

After the outliers were removed the so-called wavelet transformation was employed to filter out Gaussian noise.[40–42] (Removal of outliers was necessary because, in our experience, wavelet filtering does not deal with them successfully.) Wavelet transformation is a relatively new signal processing technique[40–42] which was developed to circumvent some problems of Fourier transformation. Instead of *sine* or *cosine* functions, a signal is decomposed into so-called wavelet functions (wavelets).[40–42] Decomposition consists of calculating a two-dimensional map of the so-called wavelet coefficients $W_\psi(a,b)$,

$$W_\psi(a,b) = \frac{1}{\sqrt{a}}\int_{-\infty}^{\infty} f(x)\psi^*\left(\frac{x-b}{a}\right)dx, \qquad (1)$$

where $\psi(x)$ is the wavelet function, $f(x)$ is the analyzed function or data set, a is the scale, and b is position (shift) parameter. Similar to Fourier filtering, wavelet filtering consists of transforming a signal to the wavelet domain, setting the small coefficients (below the appropriately chosen threshold value) to zero and performing an inverse transformation. The results of wavelet filtering applied to magneto-optical ratios are shown with red lines in Fig. 6. For the results presented, we employed wavelet packet decomposition[40–42] using symlet wavelets on the order of 3 ("sym3") and three levels of decomposition. However, it must be pointed out that similar results were obtained using other wavelets. Thresholding of wavelet coefficients was done using the so-called "soft thresholding."[40–42]

As can be seen from Fig. 6, this filtering procedure removes most of the high-frequency noise and at the same time preserves the overall shape of the ratios. The mean values and standard deviations of the data before and after processing are shown in Table II. One can note that the filtering does not change the mean values significantly but does reduce the standard deviations by a factor of approximately 5. As the final step in the analysis, we fit the filtered ratios with polynomial function of the form $f(\omega)=C_0+C_1\omega+C_2\omega^2$. Visually, we expect only C_0 term to have significant values. Indeed, the fits reveal that C_1 and C_2 are negligibly small; i.e., the ratios can be approximated with straight, horizontal lines. The values of C_0 are also shown in Table II.

The results of Fig. 6 indicate that there are no field-induced changes in any of the ratios. Based on statistical

TABLE II. The mean values and standard deviations of transmission ratios at 33 T before (μ_b and σ_b) and after (μ_a and σ_a) wavelet filtering (Figs. 4 and 6, respectively).

Kelvin	μ_b	σ_b	μ_a	σ_a	C_0
5	1.0088	0.0251	1.0116	0.0047	1.0073
15	1.0162	0.0222	1.0166	0.0057	1.0238
30	1.0212	0.0348	1.0214	0.0060	1.0211
45	1.0213	0.0206	1.0238	0.0058	1.0315

analysis we put the error bars at ±1.0%, with probability of 95%.[39] Again, we do not detect any systematic changes as a function of temperature or development of structures in transmission. However, we do note that all four curves are offset from unity (shifted vertically up). The origin of this effect is unknown at the moment, but we emphasize that it is present both below and above T_c and therefore cannot be associated with superconducting transition.

V. DISCUSSION

Mid-IR physics has long been speculated to play an important role in high-T_c cuprates.[43–45] However, various technical difficulties such as small sample size, poor resolution, or low signal-to-noise ratio have precluded more detailed experimental studies of this energy range. Recent advances in ARPES and INS, as well as IR, have brought the mid-IR physics back to the focus of attention.[10–13,15,16,46] Various features have been found in this frequency range, and their origin, as well as their relation to high-T_c superconductivity, is currently being debated. The magneto-optical results presented here put constrains on their explanations. They indicate that mid-IR features are not very susceptible to external magnetic field. No changes in optical properties were found even when driving the system from normal to superconducting states. This might also indicate that the modes are not very strongly coupled to charge carriers. It remains to be seen if any field-induced changes can be detected at lower frequencies, where they are expected because of gap closing.

One of the most enigmatic mid-IR features is the so-called "mid-IR band"[23,43–45] for which various proposals have been advocated. Leggett[45] argued that the energy of superconducting condensation is stored in the mid-IR peak.[47,48] In his model, changes in mid-IR peak are expected upon entering the superconducting state,[47] and they are also expected to result in changes in optical properties. However, within the error bars of our measurement system, we did not find any field-induced changes in transmission even in 33 T magnetic field, which is sufficient to drive optimally doped LSCO from superconducting to normal states.

To simulate the effect of magnetic field on optical properties, we have performed simple calculations based on a Drude-Lorentz (DL) model. The optimally doped LSCO film is described with a DL model, assuming a single Lorentzian in the mid IR.[49] The LSAO substrate is assumed to be nonabsorbing and described by a real dielectric function $\epsilon(\infty) \approx 4$.[36] The transmission of the two-layer system was calculated using standard equations.[37] To simulate the effect of magnetic field, the oscillator strength of the mid-IR mode is then changed by a certain amount and the transmission obtained. Finally the ratio of the two transmissions was calculated. Our experiments in 33 T put the upper bound on changes in transmission to ±1%, which on the other hand, through these simple DL calculations, puts the upper bound of about ±0.5% on the changes in the mid-IR mode.

VI. SUMMARY AND CONCLUSIONS

In summary, we performed magnetotransmission study of a series of LSCO films and did not detect any systematic field-induced changes in the mid-IR transmission in any of the samples in magnetic field of 18 T. In addition, no field-induced changes were found in an optimally doped LSCO film with T_c=41 K, even in a magnetic field as high as 33 T. Even though the exact nature of various mid-IR modes is currently unknown; these results, combined with previous magnetoreflection results,[20–23] put important constrains on the nature of these modes. For example, these results rule out coupling of mid-IR charge excitations to the so-called 41 meV resonance, which is known to be very sensitive to external magnetic field.[24,25]

ACKNOWLEDGMENTS

The authors would like to thank Yoichi Ando, D.N. Basov, C.C. Homes, and A.J. Millis for useful discussions. A portion of this work was performed at the National High Magnetic Field Laboratory, which is supported by the NSF under Cooperative Agreement No. DMR-0084173 and by the State of Florida. The work at BNL was supported by U.S. DOE under Project No. MA-509-MACA.

*dsasa@uakron.edu

[1] P. D. Johnson, T. Valla, A. V. Fedorov, Z. Yusof, B. O. Wells, Q. Li, A. R. Moodenbaugh, G. D. Gu, N. Koshizuka, C. Kendziora, Sha Jian, and D. G. Hinks, Phys. Rev. Lett. **87**, 177007 (2001).
[2] A. Lanzara, P. V. Bogdanov, X. J. Zhou, S. A. Kellar, D. L. Feng, E. D. Lu, T. Yoshida, H. Eisaki, A. Fujimori, K. Kishio, J.-I. Shimoyama, T. Noda, S. Uchida, Z. Hussain, and Z.-X. Shen, Nature (London) **412**, 510 (2001).
[3] A. Damascelli, Z. Hussain, and Z.-X. Shen, Rev. Mod. Phys. **75**, 473 (2003).
[4] J. Hwang, T. Timusk, and G. Gu, Nature (London) **427**, 714 (2004).
[5] S. V. Dordevic, C. C. Homes, J. J. Tu, T. Valla, M. Strongin, P. D. Johnson, G. D. Gu, and D. N. Basov, Phys. Rev. B **71**, 104529 (2005).
[6] E. Schachinger, D. Neuber, and J. P. Carbotte, Phys. Rev. B **73**, 184507 (2006).
[7] J. P. Carbotte, E. Schachinger, and D. N. Basov, Nature (London) **401**, 354 (1999).
[8] J. Hwang, T. Timusk, E. Schachinger, and J. P. Carbotte, Phys. Rev. B **75**, 144508 (2007).
[9] E. van Heumen, E. Muhlethaler, A. B. Kuzmenko, D. van der Marel, H. Eisaki, M. Greven, W. Meevasana, and Z. X. Shen, arXiv:0807.1730 (unpublished).
[10] B. P. Xie, K. Yang, D. W. Shen, J. F. Zhao, H. W. Ou, J. Weil, S. Y. Gu, M. Arita, S. Qiao, H. Namatame, M. Taniguchi, N. Kaneko, H. Eisaki, K. D. Tsuei, C. M. Cheng, I. Vobornik, J. Fujii, G. Rossi, Z. Q. Yang, and D. L. Feng, Phys. Rev. Lett. **98**, 147001 (2007).
[11] T. Valla, T. E. Kidd, W.-G. Yin, G. D. Gu, P. D. Johnson, Z.-H.

Pan, and A. V. Fedorov, Phys. Rev. Lett. **98**, 167003 (2007).

[12] J. Graf, G.-H. Gweon, and A. Lanzara, Physica C **460–462**, 194 (2007).

[13] J. Chang, S. Pailhes, M. Shi, M. Manson, T. Claesson, O. Tjernberg, J. Voigt, V. Perez, L. Patthey, N. Momono, M. Oda, M. Ido, A. Schnyder, C. Mudry, and J. Mesot, Phys. Rev. B **75**, 224508 (2007).

[14] Although the two might be strongly coupled.

[15] J. M. Tranquada, H. Woo, T. G. Perring, H. Goka, G. D. Gu, G. Xu, M. Fujita, and K. Yamada, Nature (London) **429**, 534 (2004).

[16] S. M. Hayden, H. A. Mook, Pengcheng Dai, T. G. Perring, and F. Dogan, Nature (London) **429**, 531 (2004).

[17] C. Stock, W. J. L. Buyers, R. A. Cowley, P. S. Clegg, R. Coldea, C. D. Frost, R. Liang, D. Peets, D. Bonn, W. N. Hardy, and R. J. Birgeneau, Phys. Rev. B **71**, 024522 (2005).

[18] N. B. Christensen, D. F. McMorrow, H. M. Ronnow, B. Lake, S. M. Hayden, G. Aeppli, T. G. Perring, M. Mangkorntong, M. Nohara, and H. Takagi, Phys. Rev. Lett. **93**, 147002 (2004).

[19] B. Vignolle, S. M. Hayden, D. F. McMorrow, H. M. Ronnow, B. Lake, C. D. Frost, and T. G. Perring, Nat. Phys. **3**, 163 (2007).

[20] H. L. Liu, A. Zibold, D. B. Tanner, Y. J. Wang, M. J. Burns, K. A. Delin, M. Y. Li, and M. K. Wu, Solid State Commun. **109**, 7 (1998).

[21] Y. S. Lee, Z. Q. Li, W. J. Padilla, S. V. Dordevic, C. C. Homes, K. Segawa, Y. Ando, and D. N. Basov, Phys. Rev. B **72**, 172511 (2005).

[22] S. V. Dordevic, C. C. Homes, G. D. Gu, W. Si, and Y. J. Wang, Phys. Rev. B **73**, 132501 (2006).

[23] Y. S. Lee, K. Segawa, Z. Q. Li, W. J. Padilla, M. Dumm, S. V. Dordevic, C. C. Homes, Y. Ando, and D. N. Basov, Phys. Rev. B **72**, 054529 (2005).

[24] Pengcheng Dai, H. A. Mook, G. Aeppli, S. M. Hayden, and F. Dogan, Nature (London) **406**, 965 (2000).

[25] B. Lake, G. Aeppli, K. N. Clausen, D. F. McMorrow, K. Lefmann, N. E. Hussey, N. Mangkorntong, M. Nohara, H. Takagi, T. E. Mason, and A. Schroder, Science **291**, 1759 (2001).

[26] I. Bozovic, IEEE Trans. Appl. Supercond. **11**, 2686 (2001).

[27] Film thickness must not be large as to render the sample non-transparent, but on the other hand it must be large enough to produce significant absorption of electromagnetic radiation. For example, for the film with $x=0.10$ the absolute value of transmission is reduced by about 50% compared with the bare substrate.

[28] The Néel temperatures for film are not available. The temperatures shown in the table are for bulk samples with similar doping levels: A. Gozar, B. S. Dennis, G. Blumberg, Seiki Komiya, and Yoichi Ando, Phys. Rev. Lett. **93**, 027001 (2004).

[29] Yoichi Ando, G. S. Boebinger, A. Passner, L. F. Schneemeyer, T. Kimura, M. Okuya, S. Watauchi, J. Shimoyama, K. Kishio, K. Tamasaku, N. Ichikawa, and S. Uchida, Phys. Rev. B **60**, 12475 (1999).

[30] Y. Wang and H.-H. Wen, Europhys. Lett. **81**, 57007 (2008).

[31] I. Bozovic, G. Logvenov, M. A. J. Verhoeven, P. Caputo, E. Goldobin, and T. H. Geballe, Nature (London) **422**, 873 (2003).

[32] I. Bozovic, G. Logvenov, M. A. J. Verhoeven, P. Caputo, E. Goldobin, and M. R. Beasley, Phys. Rev. Lett. **93**, 157002 (2004).

[33] N. Gedik, D.-S. Yang, G. Logvenov, I. Bozovic, and A. H. Zewail, Science **316**, 425 (2007).

[34] S. Kamba, E. Buixaderas, and A. Pajaczkowska, Phys. Status Solidi A **168**, 317 (1998).

[35] J. Humlicek, R. Henn, and M. Cardona, Phys. Rev. B **61**, 14554 (2000).

[36] G. X. Chen, Y. J. Ge, C. Z. Bi, X. G. Qiu, and B. R. Zhao, J. Appl. Phys. **95**, 3417 (2004).

[37] M. Dressel and G. Gruner, *Electrodynamics of Solids* (Cambridge University Press, New York, 2002).

[38] Previous IR measurements on LSAO did not detect any *temperature* dependence in this frequency range (Refs. 34–36).

[39] J. M. Chambers, W. S. Cleveland, B. Kleiner, and P. Tukey, *Graphical Methods for Data Analysis* (Wadsworth, California, 1983).

[40] G. Kaiser, *A Friendly Guide to Wavelets* (Birkhauser-Boston, Cambridge, MA, 1994).

[41] E. Hernandez and G. L. Weiss, *A First Course on Wavelets* (CRC, Boca Raton, FL, 1996).

[42] *Wavelets in physics*, edited by J. C. van den Berg (Cambridge University Press, New York, 1999).

[43] T. Timusk and D. B. Tanner, in *Physical Properties of High Temperature Superconductors I*, edited by D. M. Ginsberg (World Scientific, Singapore, 1989).

[44] T. Timusk and D. B. Tanner, in *Physical Properties of High Temperature Superconductors III*, edited by D. M. Ginsberg (World Scientific, Singapore, 1996).

[45] A. J. Leggett, J. Phys. Chem. Solids **59**, 1729 (1998).

[46] J. Hwang, E. J. Nicol, T. Timusk, A. Knigavko, and J. P. Carbotte, Phys. Rev. Lett. **98**, 207002 (2007).

[47] A. J. Leggett, Proc. Natl. Acad. Sci. U.S.A. **96**, 8365 (1999).

[48] A. J. Leggett, Nat. Phys. **2**, 134 (2006).

[49] The optical conductivity data for LSCO with similar doping level (Ref. 50) were fit with DL model, $\epsilon(\omega)=1-\frac{\omega_D^2}{\omega(\omega+i/\tau)}+\frac{\omega_L^2}{\omega_0^2-\omega^2-i\omega\gamma}$, with $\omega_D=6300$ cm^{-1}, $\tau=115$ cm^{-1}, $\omega_0=250$ cm^{-1}, $\omega_L=13000$ cm^{-1}, and $\gamma=4000$ cm^{-1}.

[50] F. Gao, D. B. Romero, D. B. Tanner, J. Talvacchio, and M. G. Forrester, Phys. Rev. B **47**, 1036 (1993).